Science Advances
AAAS

advances.sciencemag.org/cgi/content/full/4/4/eaao5864/DC1

# Supplementary Materials for

## Crystal structure and equation of state of Fe-Si alloys at super-Earth core conditions

June K. Wicks, Raymond F. Smith, Dayne E. Fratanduono, Federica Coppari, Richard G. Kraus, Matthew G. Newman, J. Ryan Rygg, Jon H. Eggert, Thomas S. Duffy

Published 25 April 2018, *Sci. Adv.* **4**, eaao5864 (2018)
DOI: 10.1126/sciadv.aao5864

**This PDF file includes:**

# SUPPLEMENTARY MATERIALS

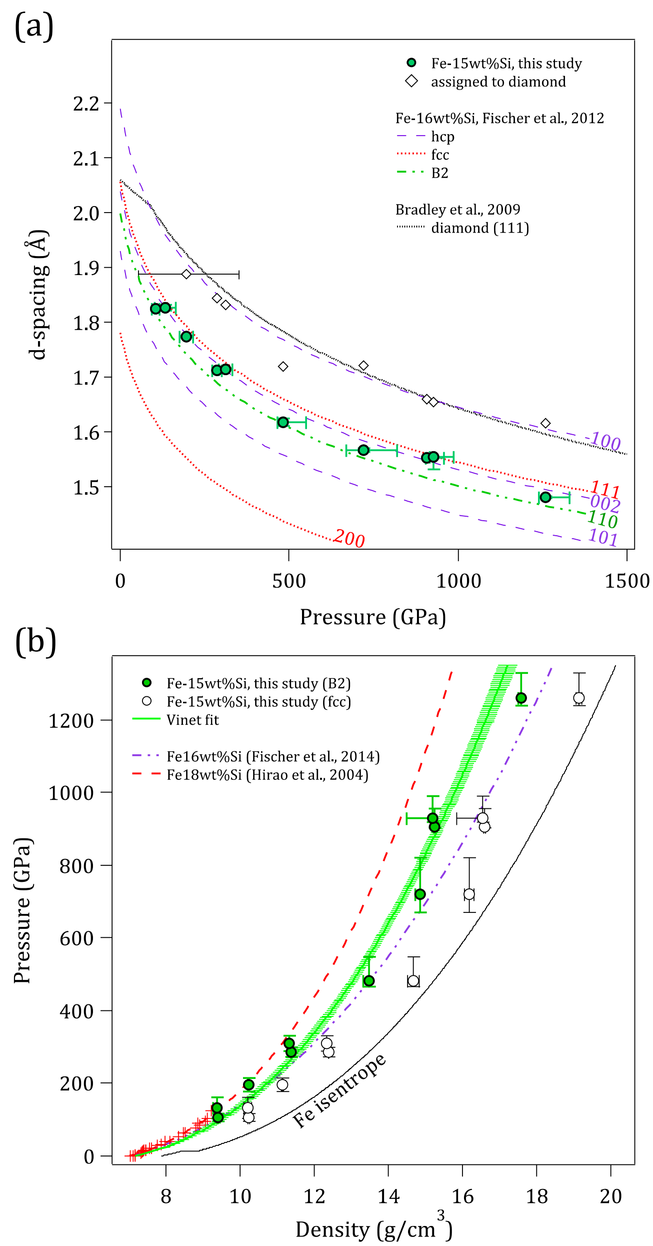


**fig. S1. Consideration of alternate structures for Fe-15Si. (a)** Comparison of *d*-spacing of candidate phases as a function of pressure. The main diffraction peak observed in Fe-15Si experiments could by itself be interpreted as $fcc_{111}$, $hcp_{002}$, or $bcc/B2_{110}$. We rule out fcc at low pressure due to the absence of the stronger 200 reflection, and at high pressure due to density considerations; We rule out $hcp_{002}$ due to the absence of the 100 and 101 reflections which are expected to have much stronger intensity. The white circles represent the single-crystal-like diffraction peak which is consistent with both diamond [111], but also might be interpreted as *hcp* [100] (e.g "*" peak in Figure 2d at 1.847 Å, also see texture contrast in fig. S4). The 1$\sigma$ error bar shown for the lowest pressure diamond point is representative of the spread in diamond pressure for all shots.

**table S1. Data summary.** Uncertainty in d-spacing includes: (i) accuracy of pinhole reference peaks fit to ideal ambient-pressure 2$\theta$ values, (ii) variation in d-spacing as a function of azimuthal angle ($\varphi$), and (iii) uncertainty in the sample – pinhole (reference plane) distance. [a]Pressure uncertainty includes experimental (as determined by the VISAR record) and systematic (uncertainty in material EOS models) contributions (see *Materials and Methods*). [b]Targets with LiF windows. [c]Lattice parameters calculated from all three *hcp* reflections.

| P(GPa)[a] | Shot No. | wt. %Si | d-spacing (Å) | | | | a (Å) | c (Å) | c/a | Density (g/cm$^3$) |
|---|---|---|---|---|---|---|---|---|---|---|
| | | | bcc (110) | hcp (100) | hcp (002) | hcp (101) | | | | |
| 140(20)[b,c] | s76622 | 7 | - | 1.9773(30) | 1.8445(25) | 1.7475(10) | 2.2857(51) | 3.6903(217) | 1.6358(72) | 10.288(52) |
| 335(7)[b,c] | s76621 | 7 | - | 1.8368(46) | 1.7204(236) | 1.6304(21) | 2.1262(108) | 3.4436(486) | 1.6691(206) | 12.578(169) |
| 377(-15,+65)[c] | s76623 | 7 | - | 1.8127(63) | 1.6939(112) | 1.6018(41) | 2.095(6) | 3.3888(367) | 1.6347(161) | 13.362(190) |
| 609(-20,+70) | s77734 | 7 | - | 1.7251(219) | - | 1.5276(11) | 1.9920(189) | 3.2879(1183) | 1.6505(582) | 15.353(311) |
| 945(-10,+60) | s77737 | 7 | - | 1.6619(86) | - | 1.4786(35) | 1.9190(148) | 3.2384(890) | 1.6875(452) | 16.795(461) |
| 1314(-40,+90) | s77740 | 7 | - | 1.6223(41) | - | 1.4447(43) | 1.8733(48) | 3.1756(456) | 1.6952(216) | 17.974(338) |
| 97(35)[b] | s77731 | 15 | 1.8245(24) | - | - | - | - | - | - | 9.402 (37) |
| 121(24)[b] | s76624 | 15 | 1.8263(65) | - | - | - | - | - | - | 9.374(100) |
| 190(10)[b] | s77735 | 15 | 1.7740(17) | - | - | - | - | - | - | 10.229(30) |
| 275(15)[b] | s76618 | 15 | 1.7118(10) | - | - | - | - | - | - | 11.385(20) |
| 277(25)[b] | s77742 | 15 | 1.7149(8) | - | - | - | - | - | - | 11.323(17) |
| 483(-17,+67) | s78430 | 15 | 1.6183(70) | - | - | - | - | - | - | 13.473(177) |
| 720(-50,+100) | s78428 | 15 | 1.5665(49) | - | - | - | - | - | - | 14.857(140) |
| 906(-1.5,+52) | s78429 | 15 | 1.5532(19) | - | - | - | - | - | - | 15.240(57) |
| 928(-10,+60) | s77739 | 15 | 1.5546(238) | - | - | - | - | - | - | 15.199(720) |
| 1260(-20,+70) | s78431 | 15 | 1.4808(31) | - | - | - | - | - | - | 17.586(108) |

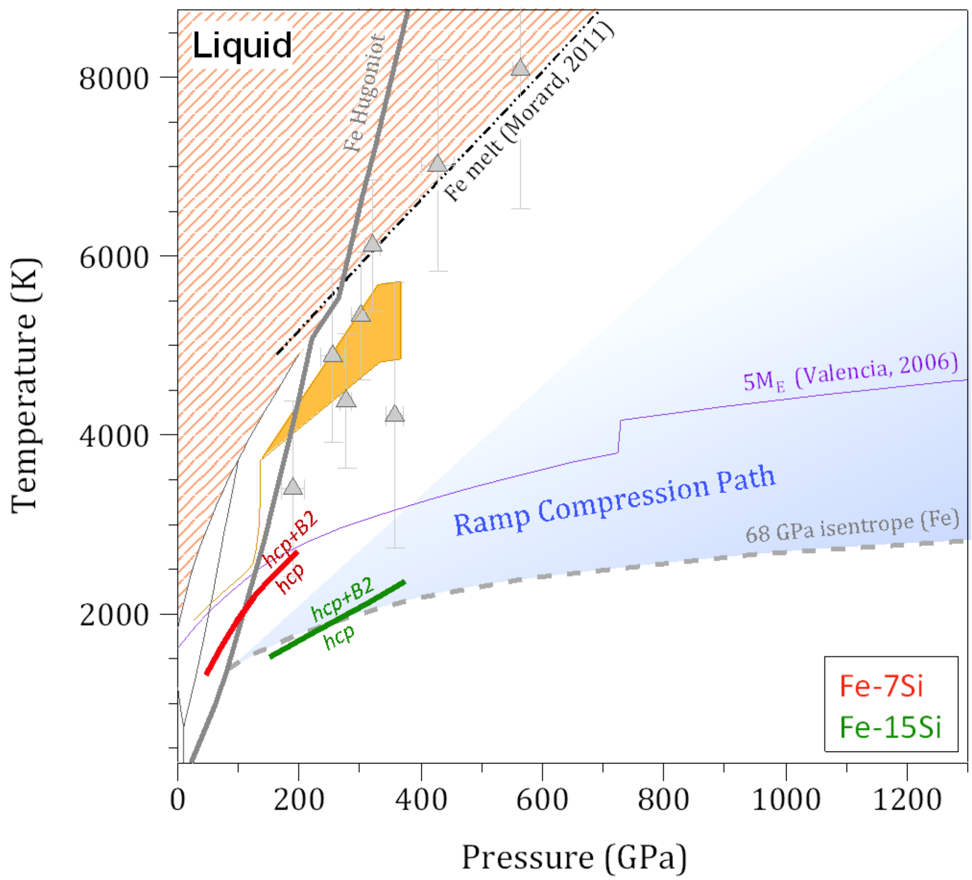


**fig. S2. Constraints on the *P-T* phase diagram for Fe-7Si and Fe-15Si.** Phase boundaries are constrained at low pressure from diamond anvil cell measurements on Fe (thin black lines) (*57*) and Fe–Si alloys, which suggest that the addition of silicon expands the stability field of the *B*2 phase with respect to that of *hcp* (*13*, *14*, *23*). Here, interpolation between measured compositions (*13*) predict the *hcp*+*B*2→*hcp* phase boundaries of Fe-7Si (bold red) and Fe-15Si (bold green). Also plotted is an example of the calculated high pressure melt line for Fe (black dash-dot-dot) (*56*) and an example of the modeled temperature profile within a 5 Earth mass rocky exoplanet (purple line) (*5*). The orange shaded region shows a range of possible temperatures for the Earth's core (*58*). The 68 GPa isentrope of Fe (bold dashed gray) represents the coolest possible *P* –*T* path in our experiments (*27*) . The approximate *P* -*T* range accessed in our ramp compression experiments (blue shaded region) is poorly constrained at high temperatures due to the unknown strength of Fe-Si under ramped compression.

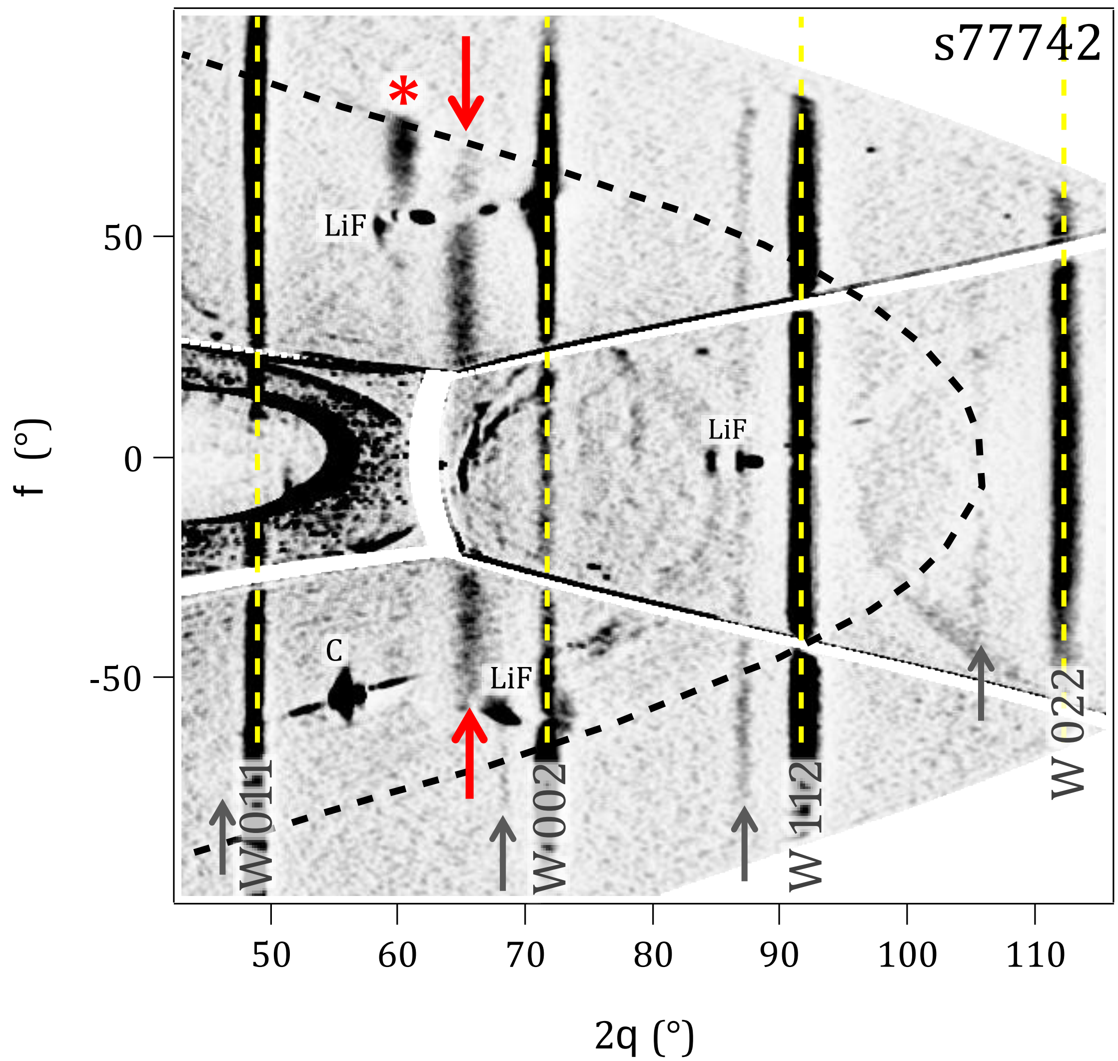


**fig. S3. Example of projected image plates, from shot s77742.** (Fe-15Si, 277±25 GPa) in $2\theta - \varphi$ coordinates (pinhole projection), where $2\theta$ is the scattering angle and $\varphi$ is the azimuthal angle about the incident X-ray beam. Yellow dashed lines correspond to diffraction from W pinhole. Diffraction peaks from less intense Fe H-$\alpha$ radiation (6.963 keV) are also observed (gray arrows). One line from the ramp compressed Fe-15Si sample is observed, consistent with a *bcc* [110] diffraction peak (red arrows). Peaks from compressed LiF and C are distinguished by texture. "*" denotes an extended feature at $2\theta$ = 60.3° which has a d-spacing consistent with both hcp [100] and diamond [111]. The black dashed curve denotes the maximum angular coverage of X-rays scattered from the sample through the 300-$\mu$m diameter, 150-$\mu m$-thick pinhole.

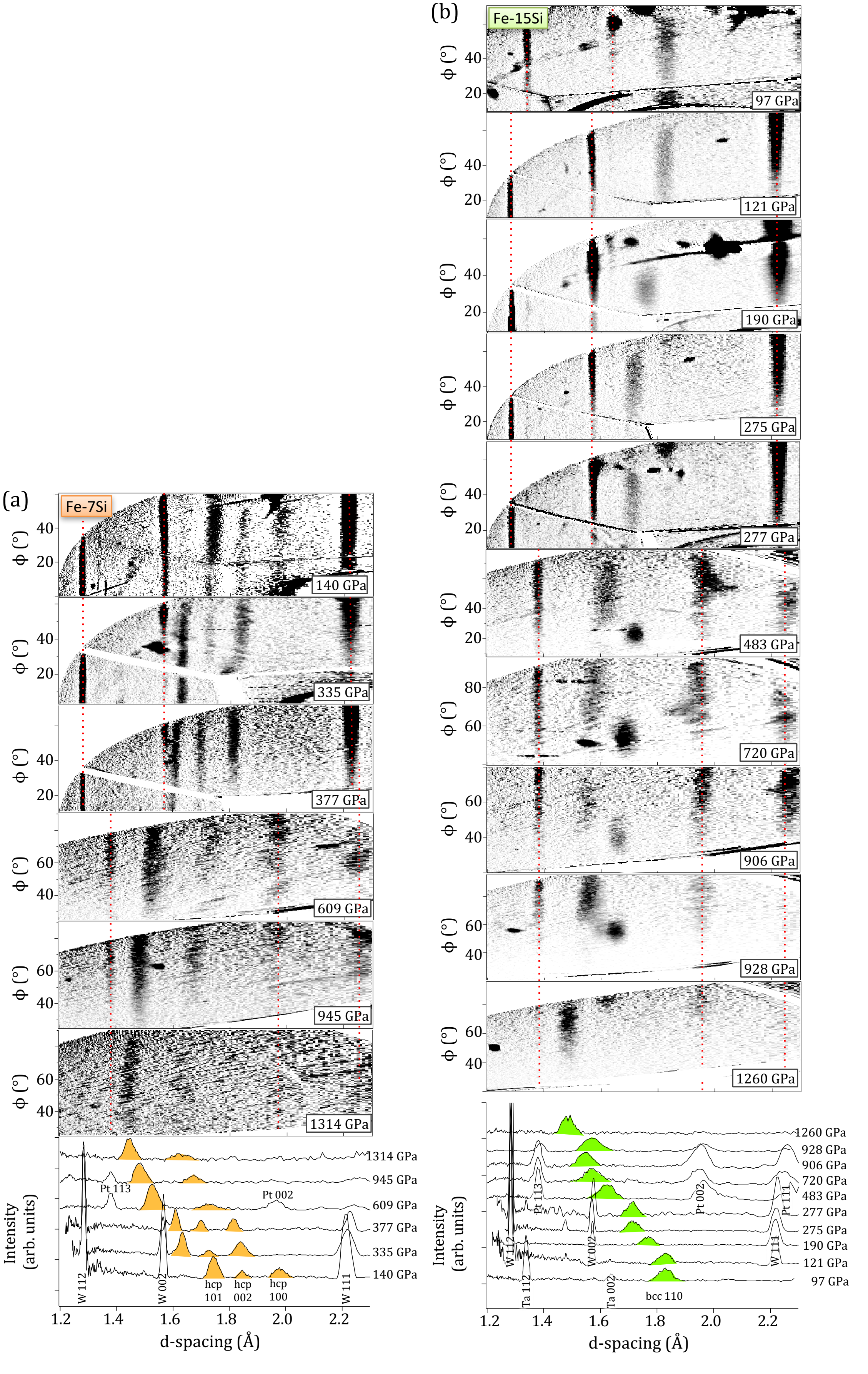

(a)
Fe-7Si
φ (°)
140 GPa
335 GPa
377 GPa
609 GPa
945 GPa
1314 GPa
Intensity (arb. units)
Pt 113
Pt 002
W 112
W 002
hcp 101
hcp 002
hcp 100
W 111
d-spacing (Å)
(b)
Fe-15Si
97 GPa
121 GPa
190 GPa
275 GPa
277 GPa
483 GPa
720 GPa
906 GPa
928 GPa
1260 GPa
Ta 112
Ta 002
bcc 110
Pt 111

**fig. S4. X-ray diffraction patterns as a function of pressure.** Each panel for **(a)** Fe-7Si and **(b)** Fe-15Si, shows a portion of the image plate projection for all shots, with sample pressure increasing from top to bottom. Vertical red dotted lines indicate diffraction from the pinhole. Diffraction peaks corresponding to Fe-Si sample in the integrated 1-d traces (bottom panels) are highlighted in orange (Fe-7Si) and green (Fe-15Si), and are summarized in table S1.

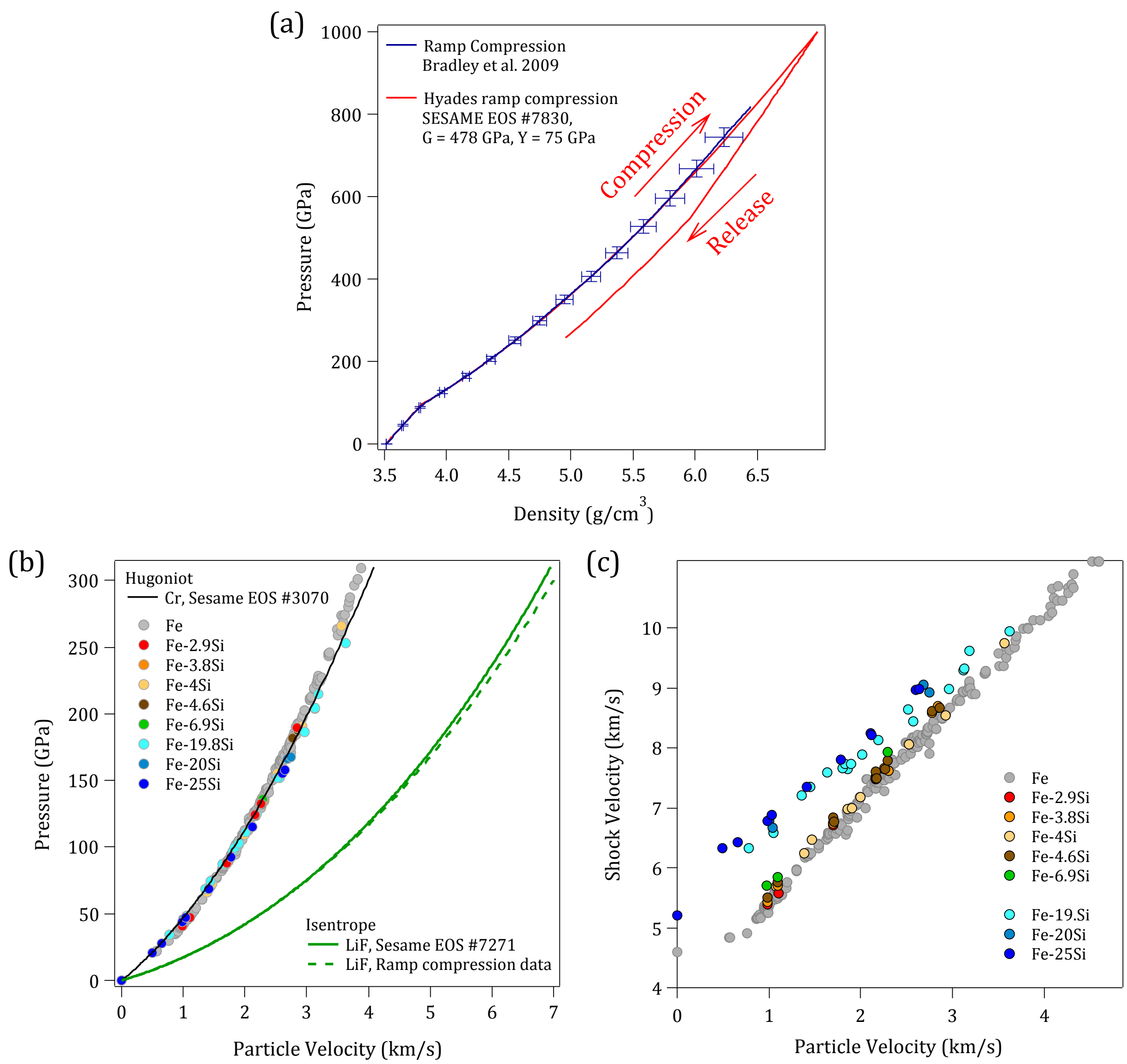


**fig. S5. Equation of state models used for pressure determination. (a)** Diamond pressure-density path measured with ramp compression (*47*) used in characteristics analysis for pressure determination in experiments with diamond windows. For comparison, the pressure-density path utilized in hydrocode simulations using a Sesame EOS (*53*) and a Steinburg-Guinan strength model (shear modulus of 478 GPa and yield stress of 75 GPa) is also shown (*59*). **(b)** Hugoniot (P-*u*) data for Fe and Fe-Si alloys (*16*, *17*, *54*, *60*, circles), and ramp compression *P*-*u* data for single crystal [100] LiF (*52*) (green dashed curve). HYADES hydrocode modeling of shots utilizing LiF windows used the Sesame EOS table #3070 to describe the *P*-*u* response of Fe-Si alloys (*53*) (Hugoniot, shown as black curve) and EOS table #7271 (Isentrope, green curve) to describe the *P*-*u* response for LiF (*53*). **(c)** Shock velocity (*Us*) versus particle velocity *u* for Fe (*54*, *60*) and Fe-Si alloys (*16*, *17*, *54*). All Fe-Si data was taken below melt. For Si concentrations from 0 → 6.9 % all the compositions exhibit a near identical *Us*-*u* slope. There is however a markedly different *Us*-*u* slope for Si concentrations > 19.8 % which suggestive of a distinct change in material compressibility for high-Si enriched samples.

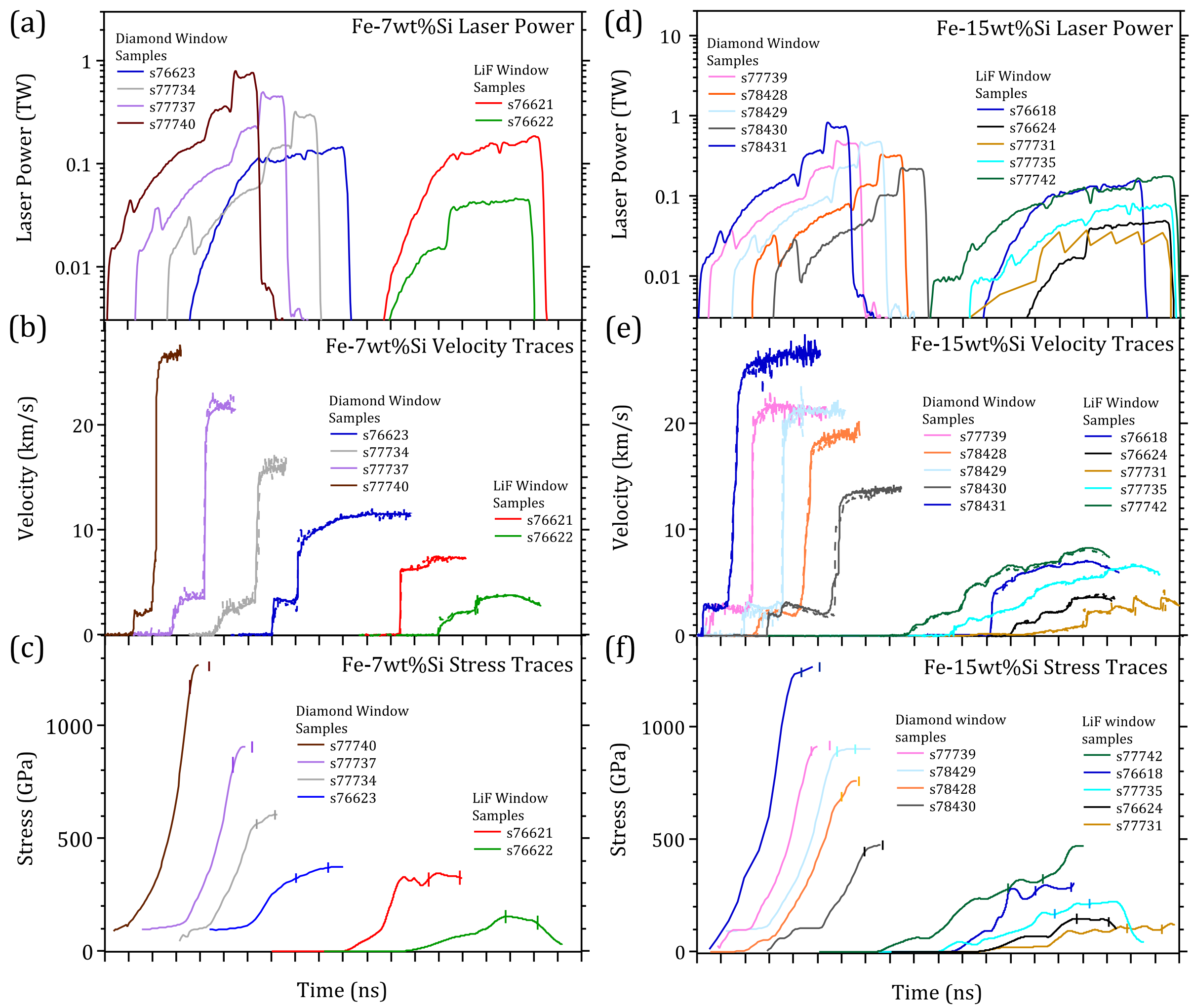


**fig. S6. Summary of laser power, interface velocity, and sample pressure history for Fe-7Si and Fe-15Si ramp-compression experiments. (a, d)** Composite laser power drive versus time. **(b, e)** Diamond free-surface velocity (left hand side) and sample-LiF interface velocity traces. **(c, f )** Calculated sample stress versus time. Vertical tick marks on traces define X-ray probe period.